



Microstructural and Chemical Evolution of $-\text{CH}_3$ -Incorporated (Low- k) SiCO(H) Films Prepared by Dielectric Barrier Discharge Plasma

Abhijit Majumdar,^{a,z} Gobind Das,^{b,d} Nainesh Patel,^b Puneet Mishra,^c
Debabrata Ghose,^c and Rainer Hippler^a

^aInstitut für Physik, Ernst Moritz Arndt Universität Greifswald, 17489 Greifswald, Germany

^bUniversità degli studio di Trento, 38100 Povo (TN), Italy

^cSurface Physics Division, Saha Institute of Nuclear Physics, 1/AF Bidhan Nagar, Kolkata 700 064, India

The present work focuses on the incorporation of $-\text{CH}_3$ radicals in organic SiCO(H) films with low dielectric constant ($k = 2.46$). The SiCO(H) films were deposited by dielectric barrier discharge plasma method using a mixture of CH_4 and Ar gases at different conditions (varying the frequency and pressure). The evolution of the film microstructure was investigated by means of X-ray photoelectron spectroscopy (XPS), Fourier transform infrared (FTIR) absorption spectroscopy, and atomic force microscopy (AFM). Various bonds, C–C, C–O, Si–O, and Si– CH_3 , were observed in XPS. In XPS analysis, it is observed that at higher frequency range (from 1 to 5 kHz), $-\text{CH}_3$ radicals (in the form of Si– CH_3) increase significantly. FTIR absorption spectra consist of several vibrational bands: namely, Si–O–Si asymmetric stretching at 1034 cm^{-1} , symmetric deformation of the $-\text{CH}_3$ group in Si– CH_3 configuration at 1270 cm^{-1} , C–H stretching of $-\text{CH}_x$ ($x = 2$ and 3) groups in the region between 3050 and 2750 cm^{-1} , and $-\text{OH}$ related vibrational bands in the range between 3700 and 3150 cm^{-1} . The change in various deposition parameters causes the change in different Si–O–Si vibrational band ratio, and the intensity of C– H_x and Si– CH_x . The film roughness was verified by AFM measurement.

© 2007 The Electrochemical Society. [DOI: 10.1149/1.2801345] All rights reserved.

Manuscript submitted August 8, 2007; revised manuscript received September 28, 2007.

Available electronically November 1, 2007.

Plasma-assisted deposition is currently the most promising field of deposition techniques, and it works in very-large scale integration (VLSI) circuits, computer chip devices, transistors, as well as in capacitor circuits.^{1,2} Reduction and structural integrity of microelectronic devices are the major challenge for circuit interconnection performances in the electrical connections between transistors. Interconnection performances are determined by the product of the resistance (R) of the metal lines and the capacitance (C) of the internal dielectrics. The signal propagation delay factor between two electronics components is important. The implementation of low-dielectric-constant (low- k) reduces the resistance–capacitance (RC) delay, power dissipation, crosstalk noise, and the number of metal levels in the electronics circuits. In order to reduce R , the transition from aluminum to copper metal lines is currently underway in the semiconductor device industry. To reduce the RC delays, low- k dielectrics are being taken into account to replace the currently used SiO_2 material for interlayer dielectric insulation. Due to the presence of organic groups (like Si– CH_3), it increases the interatomic distances in silica, which provides an additional decrease of k value (2.5–3.3).^{1,2} The structural and chemical changes on SiCO(H) films using positron annihilation spectroscopy and nuclear reaction analysis has been reported by Brusa et al.³ The control of both chemical and microstructural properties of SiCO(H) film is a challenge for the practical applications.

Hydrogenated amorphous silicon oxycarbide (SiCO/H) film can be deposited by several techniques, i.e., plasma-enhanced chemical vapor deposition (PECVD), sputtering, electron-beam evaporation, high-energy ion beam evaporation, sol-gel treatment, etc. The thin-film deposition by dielectric barrier discharge (DBD) plasma has several interesting features. It offers attractive perspectives for the coating deposition and surface functionalization as it provides an easily applicable system in the industrial process.^{4–10} The most important feature is that the plasma reaction zone is confined on the surface of the electrode or substrate area. Therefore a dielectric barrier discharge of CH_4/Ar gas mixture was employed at half the

atmospheric pressure to deposit amorphous hydrocarbon film on Si(100) wafer to study its chemical and microstructural properties.^{10,11}

In this paper, we report the use of a dielectric barrier discharge at various frequencies and at various pressure of CH_4/Ar gas mixtures in order to investigate the microstructure and chemical properties of SiCO(H) films. The chemical and structural properties of the films were investigated by means of X-ray photoelectron spectroscopy (XPS), Fourier transform infrared (FTIR) spectroscopy, and atomic force microscopy (AFM).

Experimental

SiCO(H) films are deposited on p-type Si(100) substrate by varying the pressure (300–500 mbar), CH_4/Ar gas ratio (2:1, 3:1, 4:1), and the acoustic dc frequency (1–5 kHz). The samples C14, C15, C16, C18, and C20 were deposited at constant pressure at $P = 400$ mbar with variable frequency from 1 to 5 kHz. The samples C17, C18, and C19 were deposited at constant frequency $f = 4$ kHz, with variable pressure from 300 to 500 mbar. The average power executed on the substrate during the deposition is about 5 W. From Table I, we can get the idea about the samples and DBD parameters. The experimental setup of the dielectric barrier discharge has been explained in detail elsewhere.^{10,11} The upper electrode is covered with aluminum oxide ($k \approx 10$), the lower (grounded) electrode with a glass plate ($k \approx 3.8$). Both electrodes are separated by 0.15 cm from each other. The gap between the two electrodes is variable according to the experimental requirement.

Table I. Sample number and dielectric barrier discharge parameters.

Sample no.	$\text{CH}_4:\text{Ar}$	Pressure (mbar)	Frequency (kHz)
C14	3:1	400	1
C15	3:1	400	2
C16	3:1	400	3
C17	3:1	400	4
C18	3:1	400	4
C19	4:1	500	4
C20	3:1	400	5

^d Present address: BIONEM, Facoltà di Medicina, Università “Magna Graecia” di Catanzaro, 88100 Catanzaro, Italy.

^z E-mail: majumdar@physik.uni-greifswald.de

The chamber is pumped by a membrane pump, base pressure below 10 mbar. Pressure inside the plasma chamber was controlled by two gas flow controllers for methane and nitrogen and by an adjustable needle valve between the chamber and the membrane pump. The high-voltage power supply consists of a frequency generator delivering a sinusoidal output that is fed into an audio amplifier. The amplifier can be operated at up to 500 W. Experiments were performed at 10.5 kV (peak-to-peak) and at variable frequencies.

The details regarding the calculation of capacitance (in situ dielectric constant measurement technique) are discussed in Wagner et al.¹² The capacitance of the deposited film is calculated with the help of a typical oscillographic presentation of an idealized Q-V diagram which is a so-called Lissajous figure.¹² The deposition time was typically about 2 h. The deposited films were investigated by means of the following techniques.

XPS measurements of the SiCO(H) films were performed on a VG Microtech (CLAM2: multi-technique 100 mm hemispherical electron analyser) X-ray photoelectron spectrometer using Mg K α radiation (photon energy 1253 eV) as the excitation source and the binding energy (BE) of Au (Au 4f_{7/2}: 84.00 eV) as the reference. The XPS spectra were collected in a constant analyzer energy mode, at a chamber pressure 10⁻⁸ mbar and pass energy of 23.5 eV at 0.125 eV/step.

FTIR measurements were carried out in transmission mode at room temperature in the spectral range between 4000 and 400 cm⁻¹. All the FTIR spectra were recorded with a resolution of 4 cm⁻¹ using a Si wafer as a reference. The number of scans for each spectrum was automatically chosen and averaged in order to ensure an optimal signal-to-noise ratio. A linear baseline was systematically subtracted from all the FTIR spectra in order to make the comparison among them more significant.

AFM is a powerful tool to characterize the surface morphology and to understand the surface roughness in a nanometer scale. Surface topographies of the SiCO(H) films were investigated by Nanoscope IV AFM (M/S Veeco, USA) in the tapping mode at ambient conditions, with a silicon cantilever having a sharp silicon tip. The radius of curvature of the Si tip is around 10 nm. We varied the scanning areas from 1 × 1 to 5 × 5 μm with a resolution of 512 pixels. In order to avoid an overestimation of the surface roughness resulting from the presence of a tilted plane when examining the film surface by AFM, the line-by-line flattening was made in the fast direction using nanoscope data processing software to remove such a tilted plane.

Results and Discussion

X-ray photoelectron spectroscopy (XPS).—Figure 1 shows the full-scale XPS spectrum in the BE range 50–600 eV. We found the O 1s, C 1s, Si 2p, and Si 2s peaks in the full scale of XPS spectrum of C18 film. The Si 2s peak is not discussed here because the atomic scattering factor (ASF) is too small in the case of Si 2s to perform quantitative peak analysis by the spectral deconvolution method. Si/C and Si/O ratios of the deposited films were measured by XPS for three the samples. The measured Si/C and Si/O ratios for various samples, C17, C18, and C19, are 0.2, 0.29, and 0.34 and 0.95, 0.85, and 0.87, respectively. Chemical bonds among carbon, silicon, and oxygen can be deduced from a deconvolution of individual Si 2p, C 1s, and O 1s lines into Gaussian line shapes.^{13–15} In order to minimize the interference between the peaks during deconvolution, all spectra have been fitted with equal linewidths (full width at half-maximum, fwhm) of the concerned individual peak, thereby reducing the number of free parameters and yielding a more stable result. All fittings were obtained by constraining the fwhm to be equal to 1.86 eV.

We considered that the surface spectrum was influenced by adsorbed molecules (e.g., oxygen, hydrogen). The investigated Si 2p, C 1s, and O 1s spectra displayed a chemical shift caused by an anomalous behavior of the surface charge distribution of the silicon substrate covered by carbon film. Si 2p with BE = 99.50 eV was

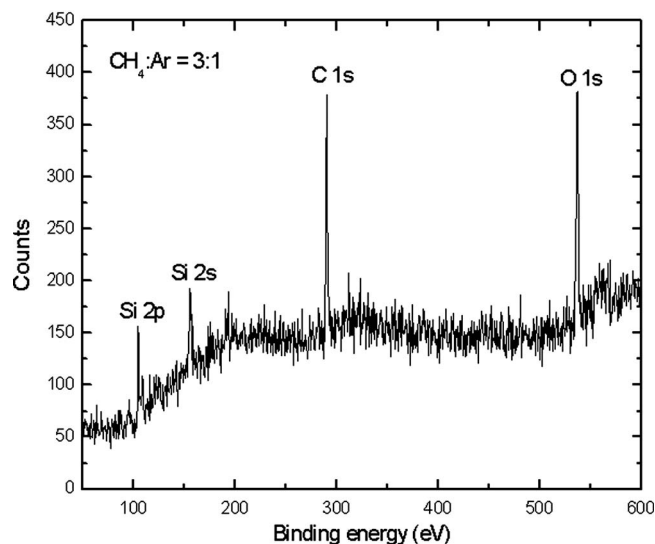


Figure 1. Full-scale XPS spectrum of the deposited polymer films when CH₄/Ar = 3:1 (C18) ($f = 4$ kHz, $P = 400$ mbar).

taken as reference, as shown in Fig. 2a. A small part of the deposited film was removed in order to get access to the Si surface. A shift of 5.0 ± 0.5 eV was noted. The results presented below have been corrected for all the spectra by subtracting the experimentally observed shift.¹⁶ The deconvoluted Si 2p spectra exhibit two peaks at 99.50 and 100.26 eV which are assigned to Si and Si–O bonds.¹⁶ Typical C 1s and O 1s spectra are displayed in Fig. 2b and c. The C 1s spectrum exhibits three peaks at 284.00, 284.85, and 286.50 eV, which have been attributed to Si–(CH₃)_x, C–C, and C–O(H) bonds, respectively.^{13,15,17} Similarly, the deconvoluted O 1s spectrum shows two peaks at 531.65 and 532.64 eV, which have been assigned to C–O(H) and Si–O bonds, respectively.^{13,14,18}

From Fig. 3a, we can see that as the frequency increases from 1 to 5 kHz the Si/C ratio decreases correspondingly. From Fig. 3a, we can see that the relative intensity of the Si/O band shows its decreasing tendency as the frequency increases from 1 to 5 kHz. In particular, the Si/C curve shows a slightly larger variation from 3 to 5 kHz, compared to Si/O. Part of the oxygen is directly connected to Si substrate (in the form of Si–O, SiO₂, or SiO₄), and the rest is coming from contamination with the air. The elevated frequency increases the flux of the –CH₃ radicals toward the Si surface during the plasma discharge. Increase of flux (frequency) signifies the increase in the density of carbon and hydrogen atoms toward the Si substrate which dominates the surface phase reaction. As a result, a hydrocarbon layer covers the major part of the Si substrate. The experiments were performed at room temperature under a pressure of 300–500 mbar.

Figure 3b depicts the quantitative analysis of the three peaks [Si–(CH₃)_x, C–C, and C–O(H) bonds] of the film, keeping a CH₄–Ar = 3:1 gas mixture and varying the frequency. From Fig. 3b, we can see that the Si–CH₃ band increases and the C–C band decreases as the acoustic frequency increases from 1 to 5 kHz. This implies that the elevated frequency causes the increase in chemical reactivity to the carbon and causes silicon atoms to bind together chemically. Alternatively, elevation of the frequency effects the incorporation of –CH₃ radicals in the deposited SiCO(H) film by CH₄/Ar DBD plasma. The C–O(H) bond remains invariant with the increase of frequency.

FTIR absorption spectroscopy.— FTIR absorption measurements for SiCO(H) samples were performed in the range between 4000 and 400 cm⁻¹. The FTIR spectra have been categorized in two parts: (i) for the samples with the increase in frequency while keep-

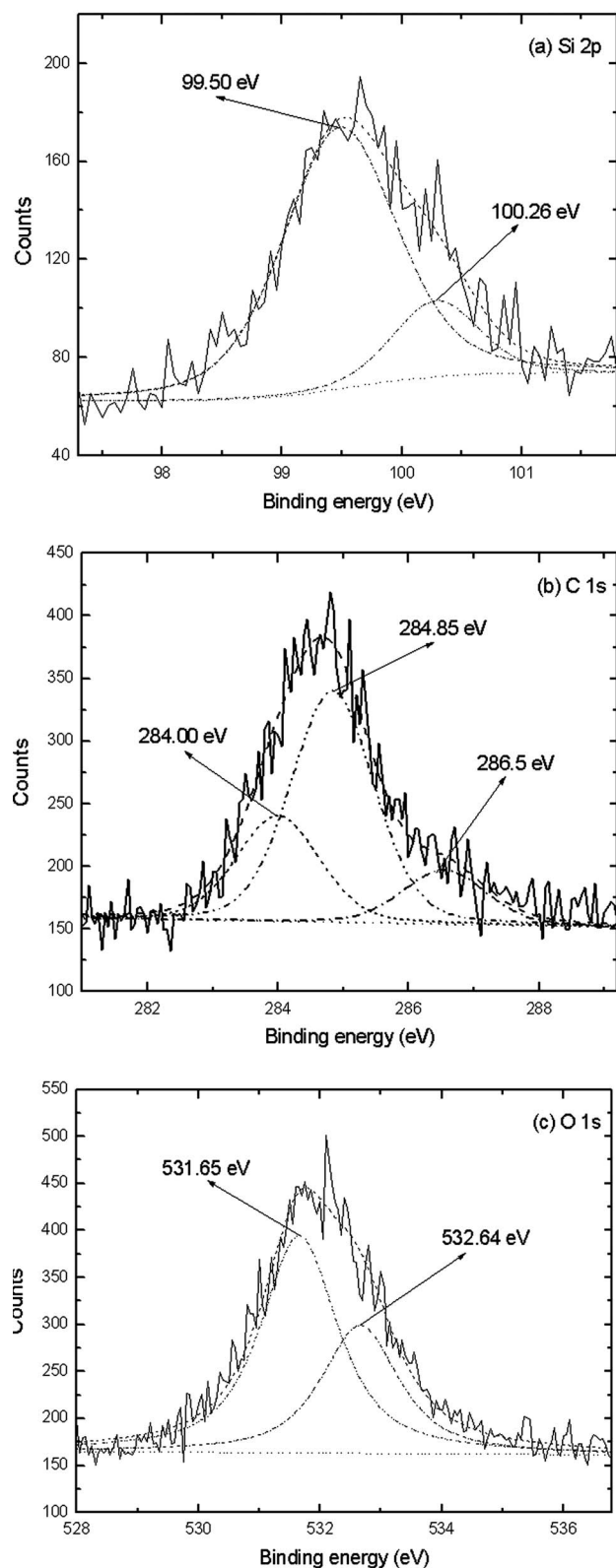


Figure 2. (a) Si 2p XPS spectra of partly removed SiOC(H) film on Si substrate (C18) (see text). (b) Typical C 1s and (c) O 1s spectra of SiOC(H) films ($\text{CH}_4/\text{Ar} = 3:1$, $\text{Si}/\text{C} = 0.34$, $f = 3$ kHz, $P = 400$ mbar).

ing the CH_4/Ar gas flow ratio, pressure, and voltage invariable, and (ii) for the samples produced by varying the pressure and keeping the voltage and frequency equal.

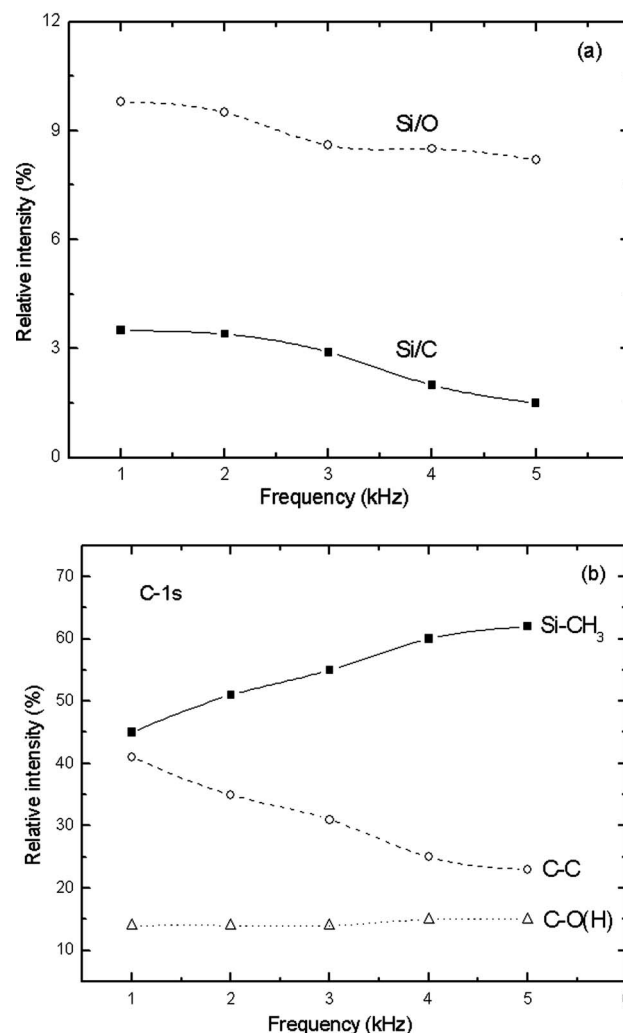


Figure 3. (a) The silicon to carbon (Si/C) and silicon to oxygen (Si/O) ratio vs frequency obtained from XPS analysis of deposited SiOC(H) films. (b) Decomposition of C 1s spectrum of SiOC(H) films into three Gaussian peaks.

Samples produced by varying the frequency.— The FTIR results of sample SiC-C14, C15, C16, and C18 are shown in Fig. 4a and b within the range between $1400\text{--}650\text{ cm}^{-1}$ and $3050\text{--}2900\text{ cm}^{-1}$. The presence of some common bands or groups of bands occurring along the overall spectral range of specific vibrational modes whose assignment is straightforward can be found in the literature.² The spectra are normalized with respect to the maximum absorbance in the range of $1150\text{--}1030\text{ cm}^{-1}$ to illustrate the evolution of various Si-O-Si, Si-CH_x, Si-C, and C-H_x content within films. The bands in the range $900\text{ to }780\text{ cm}^{-1}$, $1220\text{ to }990\text{ cm}^{-1}$, $1350\text{ to }1250\text{ cm}^{-1}$ and $3020\text{ to }2930\text{ cm}^{-1}$ can be attributed to a complex region,¹⁹ different Si-O-Si asymmetric stretching,^{2,20} Si-CH_x stretching, and C-H_x stretching vibrational bands,²¹ respectively.

Figure 4a describes the evolution in the microstructural variation with the acoustic dc frequency. It shows in the entire region that there is a sudden modification in the chemical structure of the film upon changing the frequency from 1 to 2 kHz. Afterward the change in frequency follows a systematic trend. Because the $900\text{--}780\text{ cm}^{-1}$ range is complex, we will not discuss this region in the present work. The figure shows that the increase in dc frequency from 1 kHz to 2 kHz causes a drastic change in Si-O-Si chemical bonds. It is also observed from the figure that the Si-O-Si asymmetric stretching vibrational band at 1100 cm^{-1} increases sharply

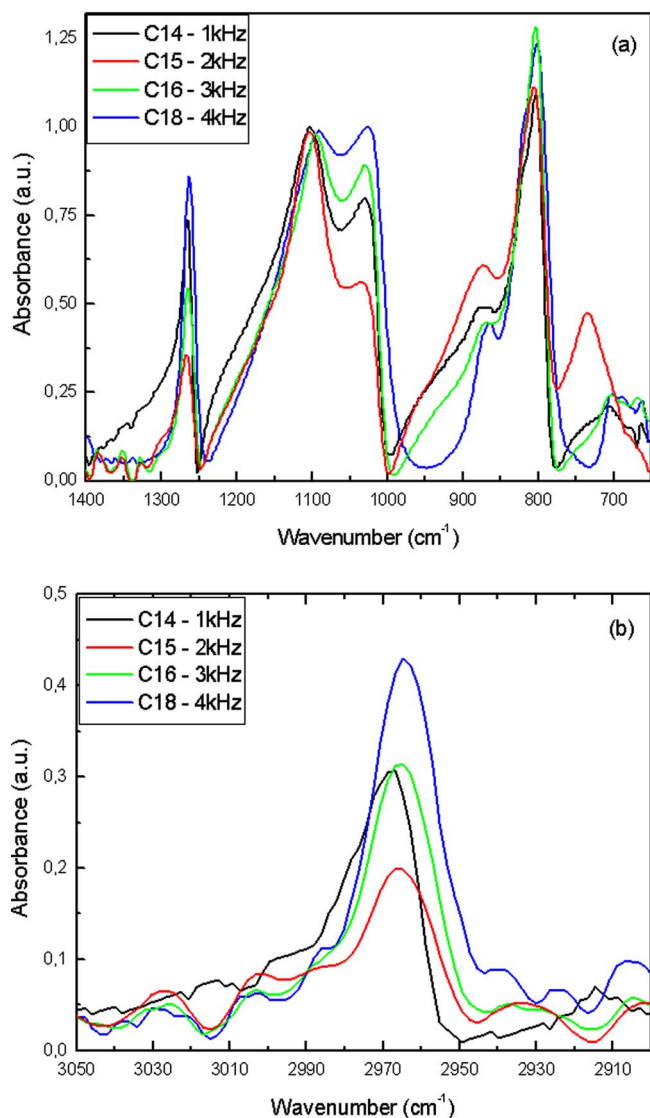


Figure 4. (Color online) (a) FTIR spectra for the samples C14, C15, C16, and C18 (increase in acoustic dc frequency) in the range between 1400 and 650 cm^{-1} and (b) in the range between 3050 and 2900 cm^{-1} .

with respect to the Si–O–Si stretching band at 1030 cm^{-1} for 2 kHz frequency with respect to the film produced at 1 kHz frequency. The high-frequency Si–O–Si band at around 1100 cm^{-1} is related to a cage structure with bond angle higher than 144° , whereas the Si–O–Si band at around 1030 cm^{-1} is due to the network structure.² The relative peak height of 1030 cm^{-1} with respect to the band around 1100 cm^{-1} increases with the increase of dc frequency, which suggests the formation of more networks structured within the film. The band in the range between 1400 and 1250 cm^{-1} clearly shows evolution of the Si–CH_x stretching band with dc frequency. This band shows the maximum intensity for sample C-18, which is deposited at higher dc frequency. A similar trend is also observed for the C–H_x stretching band in the range of 3050 – 2900 cm^{-1} , as shown in Fig. 4b. Because the increase in frequency enhances the flux of CH₃ radicals toward the Si surface, the increase in the formation of Si–CH_x and C–H_x bonds is expected within the film. The FTIR findings fully support this phenomenon (Fig. 4b).

Samples produced by varying the chamber pressure.— Figure 5 shows the absorption spectra for the samples produced by varying the CH₄/Ar gas ratio. The spectra show the vibrational bands similar to those described above. The spectra show that the change in gas

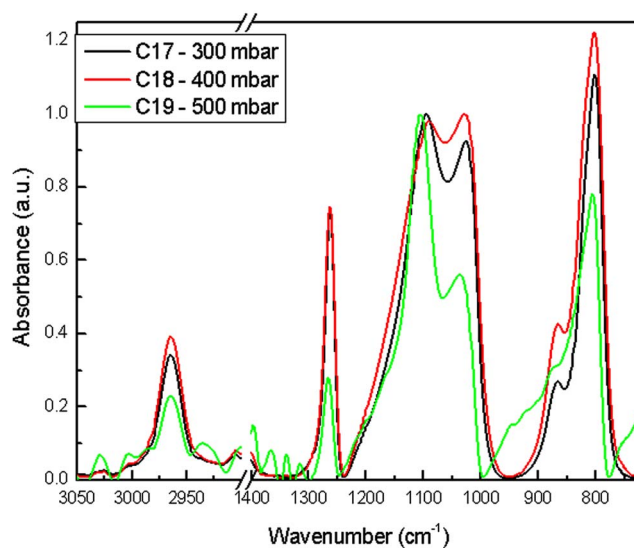


Figure 5. (Color online) FTIR absorption spectra for the samples C17, C18, and C19 in the range between 3050 and 650 cm^{-1} .

chamber pressure from 300 to 400 mbar does not change the chemical bonding on the Si substrate, but a drastic change is observed at a pressure of 500 mbar. The decrease in relative intensity of 1030 cm^{-1} vibrational band with respect to the 1100 cm^{-1} band and reduction in peak height of Si–CH_x and C–H_x are observed with the increase in chamber pressure, which could be due to the reduction in network structure and the formation of fewer Si–CH_x and C–H_x bonds within the film.

AFM.— Figures 6a and b illustrate typical three-dimensional (3D) $5 \times 5\ \mu\text{m}$ scan topographies of several SiCO(H) films with different CH₄/Ar mixtures. The film deposited at frequency $f = 5\text{ kHz}$ shows the discrete 3D island growth with root mean square (rms) roughness of 1.308 nm , whereas at $f = 1\text{ kHz}$ the rms roughness is about 0.469 nm . The average size of the islands as measured from the sectional profile typically ranges between 30 and 40 nm for a CH₄/Ar mixture at $f = 5\text{ kHz}$. As the frequency decreases, the islands gradually flatten down and the surface becomes smoother. The surface roughness of the underlying Si substrate is about 0.2 – 0.3 nm , whereas the roughness of the film in the plateau region is about 1.308 nm (in the case of $f = 5\text{ kHz}$), indicating that the gradual increase in acoustic frequency (from 1 to 5 kHz) plays an important role in increasing the surface rms roughness of the deposited SiCO(H) film. The roughness property of the films deposited by CH₄/Ar DBD plasma is comparable with the film resulting from plasma-enhanced chemical vapor deposition (PECVD), (rms roughness below 1 nm).²² Apparently, more deposition occurs in the valleys of the Si surface than on the crests. This also indicates that plasma ions injected into the growing films tend to grow atomically rough films.

Conclusion

We successfully deposited organic SiCO(H) polymer films with dielectric constant $k \approx 2.46$ by a CH₄/Ar dielectric barrier discharge plasma technique. The chemical, microstructural evolution, and the surface morphology of the films were investigated by various techniques.

The XPS spectra showed various peaks which can be attributed to Si–(CH₃)_x, C–C, and C–O(H) bonds in the C 1s spectrum. At higher frequency (from 1 to 5 kHz) the Si/O and Si/C ratios decrease gradually, which indicates that the bulk Si is covered by deposited hydrocarbon (mostly –CH₃ radical) film. The incorporation of –CH₃ radicals in SiCO(H) film is statistically significant from the XPS results. The FTIR absorption spectra show different

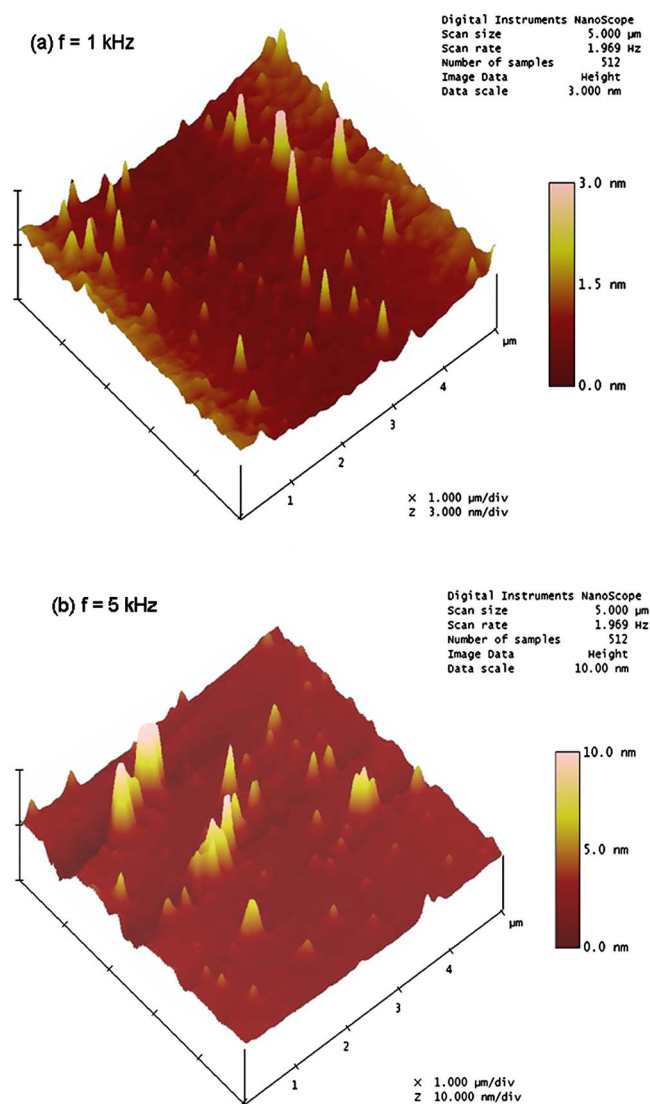


Figure 6. (Color online) 3D AFM images of SiOC(H) films on Si substrate: (a) $\text{CH}_4/\text{Ar} = 2:1$ (C17) and (b) $\text{CH}_4/\text{Ar} = 4:1$ (C19).

vibrational bands related to the Si–O–Si, Si–CH_x, and C–H_x. FTIR findings (Fig. 4b) fully support the XPS observations (Fig. 3b) with the observation that the increase in frequency causes the formation of –CH_x radicals which are responsible for reducing the dielectric constant of SiCO(H) film. The polymer film SiCO(H), deposited by CH₄/Ar DBD plasma, offers a smooth and compact surface with average roughness about 1.308 nm.

Acknowledgments

Part of this work was supported by the Deutsche Forschungsgemeinschaft (DFG) through Sonderforschungsbereich SFB/TR 24 “Fundamentals of Complex Plasmas,” and by The International Max Planck Research School (IMPRS) “Bounded Plasmas.” The authors also thankful to Dr. Aniruddha Sengupta, Max-Planck Institute, Greifswald, Germany, for several discussions.

Ernst Moritz Arndt Universitat Greifswald assisted in meeting the publication costs of this article.

References

1. K. Maex, M. R. Baklanov, D. Shamiryan, F. Iacopi, S. H. Brongersma, and Z. S. Yanovitskaya, *J. Appl. Phys.*, **93**, 8793 (2003).
2. A. Grill and D. A. Neumayer, *J. Appl. Phys.*, **94**, 6697 (2003).
3. R. S. Brusa, M. Spagolla, G. P. Karwasz, A. Zecca, G. Ottaviani, F. Corni, M. Bacchetta, and E. Carollo, *J. Appl. Phys.*, **95**, 2348 (2004).
4. G. Borcia, C. A. Anderson, and N. M. D. Brown, *Surf. Coat. Technol.*, **201**, 3074 (2006).
5. A. Sonnenfeld, T. M. Tun, L. Zajikova, K. M. Kozlov, H. E. Wagner, J. F. Behnke, and R. Hippler, *Plasmas Polym.*, **6**, 237 (2001).
6. O. Goossens, E. Dekempeneer, D. Vangeneugden, R. Van De Leest, and C. Leys, *Surf. Coat. Technol.*, **142**, 474 (2001).
7. S. Paulussen, R. Rego, O. Goossens, D. Vangeneugden, and K. Rose, *J. Phys. D.*, **38**, 568 (2005).
8. Y. H. Liu, J. Li, D. P. Liu, T. C. Ma, and G. Benstetter, *Surf. Coat. Technol.*, **200**, 5819 (2006).
9. P. Heyse, R. Dams, S. Paulussen, K. Houthoofd, K. Janssen, P. A. Jacobs, and B. F. Sels, *Plasma Processes Polym.*, **4**, 145 (2007).
10. A. Majumdar and R. Hippler, *Rev. Sci. Instrum.*, **78**, 075103 (2007).
11. A. Majumdar, J. F. Behnke, R. Hippler, K. Matyash, and R. Schneider, *J. Phys. Chem. A*, **109**, 9371 (2005).
12. H. E. Wagner, R. Brandenburg, K. V. Kozlov, A. Sonnenfeld, P. Michel, and J. F. Behnke, *Vacuum*, **71**, 417 (2003).
13. J. Heo and H. J. Kim, *J. Electrochem. Soc.*, **153**, F228 (2006).
14. M. R. Alexander, R. D. Short, F. R. Jones, W. Michaeli, and C. J. Blomfield, *Appl. Surf. Sci.*, **137**, 179 (1999).
15. E. Riedo, F. Comin, J. Chevrier, F. Schmithusen, S. Decossas, and M. Sancrotti, *Surf. Coat. Technol.*, **125**, 124 (2000).
16. A. Majumdar, J. Schäfer, P. Mishra, D. Ghose, J. Meichsner, and R. Hippler, *Surf. Coat. Technol.*, **201**, 6437 (2007).
17. L. M. Han, J. S. Pan, S. M. Chen, N. Balasubramaniam, J. Shi, L. S. Wong, and P. D. Foo, *J. Electrochem. Soc.*, **148**, F151 (2001).
18. X. Yan, T. Xu, G. Chen, S. Yang, H. Liu, and Q. Xue, *J. Phys. D.*, **37**, 907 (2004).
19. G. Socrates, *Infrared Characteristic Group Frequencies*, p. 186, John Wiley & Sons, Chichester (1994).
20. T. C. Chang, Y. S. Mor, P. T. Liu, T. M. Tsai, C. W. Chen, C. J. Chu, F. M. Pan, W. Lur, and S. M. Sze, *J. Electrochem. Soc.*, **149**, F145 (2002).
21. G. Das, G. Mariotto, and A. Quaranta, *J. Electrochem. Soc.*, **153**, F46 (2006).
22. M. E. Ramsey, E. Poindexter, J. S. Pelt, J. Marin, and S. M. Durbin, *Thin Solid Films*, **360**, 82 (2000).